Vegetation History and Archaeobotany (2018) 27:649–664
https://doi.org/10.1007/s00334-017-0663-6

ORIGINAL ARTICLE

# Millennial multi-proxy reconstruction of oasis dynamics in Jordan, by the Dead Sea

**Sebastian Eggenberger[1] · Erika Gobet[1] · Jacqueline F. N. van Leeuwen[1] · Christoph Schwörer[1] · Willem O. van der Knaap[1] · Han F. van Dobben[2] · Hendrik Vogel[3] · Willy Tinner[1] · Claire M. C. Rambeau[1,4]**

Received: 4 April 2017 / Accepted: 7 December 2017 / Published online: 18 December 2017


## Abstract

Vegetation reconstructions in the Dead Sea region based on sediment records are potentially biased, because the vast majority of them derive from the western side of the sea, and only focus on large areas and time spans, while little is known about extra-local (< 1,000 m radius) to local (< 20 m radius) changes. To fill this gap, we compared a vegetation survey with modern pollen assemblages from the "Palm Terrace" oasis ca. 300 m b.s.l. (below sea level), at the eastern edge of the Dead Sea. This revealed how the oasis vegetation is reflected in pollen assemblages. In addition, two sediment cores were collected from the centre and the edge of a mire at the oasis to reconstruct past vegetation dynamics. We analysed sedimentary pollen and microscopic charcoal, as well as the sediment chemistry by X-ray fluorescence (XRF) and conductivity, focusing on the past ~ 1,000 years. Pollen results suggest that mesophilous *Phoenix dactylifera* (date palm) stands and wetland vegetation expanded there around AD 1300–1500 and 1700–1900. During the past ca. 100 years, drought-adapted Chenopodiaceae gained ground, partly replacing the palms. Results from elemental analysis, especially of elements such as chlorine, provide evidence of enhanced evaporative salinization. Increasing desertification and the associated decline of mesophilous date palm stands during the past ca. 50 years is probably related to a decrease in annual precipitation and also corresponds to decreasing water levels in the Dead Sea. These have mainly been caused by increasing extraction of fresh water from tributaries and wells, mainly for local agriculture and industry. In the future, with hotter and drier conditions as well as increased use of water, oasis vegetation along the Dead Sea might be at further risk of contraction or even extinction.

**Keywords** Pollen · Fire history · Global change · Vegetation · XRF · *Phoenix dactylifera*

## Introduction

The Dead Sea basin is situated in the Dead Sea Transform (DST), a series of faults that shape the geology and geomorphology of the area (Garfunkel and Ben-Avraham 1996). With a water level of 430 m b.s.l. (below sea level) in 2015 (Yechieli et al. 2016), the Dead Sea is the lowest-lying water body on Earth. Its unique location combined with an extreme climate and ancient cultural legacies give special importance to this region. Whereas the whole Arabian Peninsula currently suffers from water scarcity due to the increasing water demands of growing populations (Odhiambo 2017), in Jordan this trend has been aggravated by massive immigration waves from neighbouring countries such as Syria and Iraq (Chen and Weisbrod 2016). It is therefore crucial to understand the various processes coupled to the hydrological cycles that may affect land use and vegetation dynamics.

Communicated by T. Litt.

**Electronic supplementary material** The online version of this article (https://doi.org/10.1007/s00334-017-0663-6) contains supplementary material, which is available to authorized users.

✉ Christoph Schwörer
christoph.schwoerer@ips.unibe.ch

[1] Institute of Plant Sciences and Oeschger Centre for Climate Change Research, University of Bern, Altenbergrain 21, 3013 Bern, Switzerland

[2] Wageningen University and Research, PO Box 47, 6700 AA Wageningen, The Netherlands

[3] Institute of Geological Sciences and Oeschger Centre for Climate Change Research, University of Bern, Baltzerstrasse 1+3, 3012 Bern, Switzerland

[4] Institute of Earth and Environmental Sciences, University of Freiburg, Albertstraße 23b, 79104 Freiburg im Breisgau, Germany

In the Dead Sea region, available palynological studies mainly focus on the western, Israeli side (Baruch 1993; Heim et al. 1997; Neumann et al. 2007, 2009, 2010; Leroy 2010; Leroy et al. 2010; Litt et al. 2012; Langgut et al. 2014, 2015), whereas research on the eastern, Jordanian, side is scarce (Rambeau 2010). The vegetation at the edge of the Dead Sea is characterized by striking differences in composition within small distances (Davies and Fall 2001). Our comparison of surface pollen with vegetation surveys of a small (~ 2 ha) oasis, in this study called "Palm Terrace", allows us to investigate how extra-local (< 1,000 m radius) to local (< 20 m radius; Jacobson and Bradshaw 1981) vegetation patterns are reflected in recent pollen assemblages. This comparison is used to refine the palynological vegetation reconstructions from two sediment cores from "Palm Terrace", core PT1 from the central part and core PT2 from the edge of today's wetland. In order to gain a better understanding of past environments, sedimentological proxy evidence from X-ray fluorescence (XRF) and conductivity measurements was included. The aim of this study is to provide new insights into the palaeo-environmental dynamics at the oasis over the past approximately 1,000 years. This time period is under-investigated in the region, since most published studies do not reach to the present or are too coarse in time resolution for detailed interpretation. We briefly discuss the implications of our study for global change biology and the future of desert oases.

## Study site

"Palm Terrace" (PT) is a small ~ 2 ha oasis located in northwestern Jordan (31°32′14″N, 35°33′45″E, 290–335 m b.s.l.) in the governorate of Madaba (Fig. 1). It is situated 700 m east of the Dead Sea shore (northern basin), 7 km south of the hot springs of 'Ain ez-Zara' (ancient Greek: Kallirrhoë), and 8 km north of Wadi Mujib. The site is part of the Mujib Biosphere Reserve, the lowest-lying nature reserve on Earth, established in 1985 by the Jordanian Royal Society for the Conservation of Nature. Sources from Roman historians and rabbinical traditions, as well as archaeological findings from Kallirrhoë, prove human activities in the close surroundings of the oasis during the centuries around the year AD, as well as during the early Byzantine period in the fourth and fifth century AD (Clamer 2010). On the famous mosaic map from Madaba dating from the sixth century AD, Kallirrhoë is labelled ΘΕΡΜΑΚΑΛΛΙ ΡΟΗC and Wadi Mujib can be recognised (Hirschfeld 2006). The two palms depicted in between might represent the "Palm Terrace" oasis (Fig. 2).

Tectonically, the oasis is situated on a fault parallel to the Dead Sea Transform (DST) (Garfunkel and Ben-Avraham 1996), and traces of faulting can be observed on the escarpment. This rises on the eastern side of the oasis as a steep slope of sandstone that reaches over 1,000 m a.s.l., where it merges into the Madaba and Dhiban plateaus. Whereas the spring from 'Ain ez-Zara' is fed by water from an aquifer complex in the western highlands 20–30 km further east (Salameh and Udluft 1985; Rimawi and Salameh 1988; Sawarieh et al. 2004, 2009), it is not yet clear where the

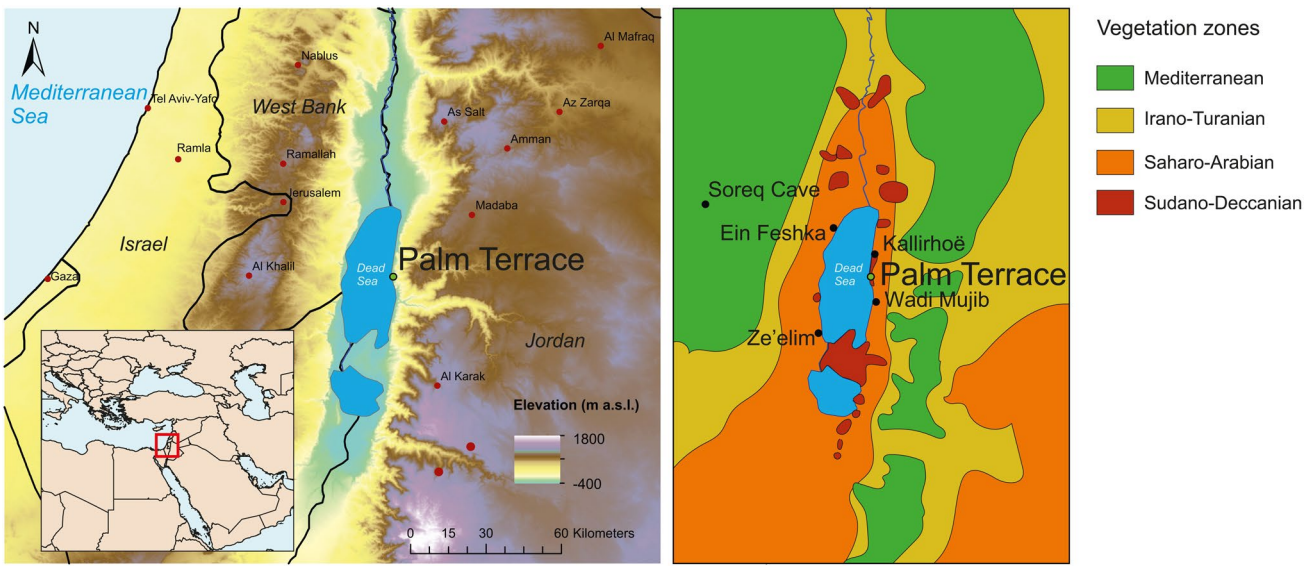


**Fig. 1** Left: Topographical map of the southern Levant showing the Dead Sea and the location of the study site "Palm Terrace". Inset shows the location of the study site in the Middle East. Right, map showing the vegetation zones in the area (after Zohary 1962; Langgut et al. 2015) and important palaeoclimatological and archaeological sites in the region


**Fig. 2** Detail of mosaic map from the sixth century AD in St. Georges Church in Madaba, Jordan. Note the broad river Jordan (1) entering the Dead Sea from the north. On the east shore of the Dead Sea, south of Kallirrhoë (2; ΘΕΡΜΑΚΑΛΛΙ ΡΟΗC) and north of Wadi Mujib (3), are two palms that might represent our study site "Palm Terrace" (4)

water of "Palm Terrace" originates from. Today's climate is characterized by extremely dry and hot conditions. Average annual rainfall over the Dead Sea is ~ 90 mm, most of which falls between October and May (Dayan and Morin 2006). The mean annual temperature is 25.9 °C, the hottest month being August with an average of 32.9 °C, the coldest January with 18.3 °C (Hect and Gertman 2003). Steep slopes combined with harsh climatic conditions make the eastern Dead Sea coast unfavourable for inhabitation. As a result of the topography, climatic gradients are also steep, creating strong environmental gradients and clear associated vegetation belts (Fig. 1, Zohary 1962; Davies and Fall 2001; Neumann et al. 2010; Langgut et al. 2015). The highest belt, the Mediterranean zone, occurs about 20 km east of the Dead Sea on the Madaba and Dhiban plateaus and is characterized by evergreen maquis scrub with *Quercus calliprinos* (evergreen oak) and *Juniperus phoenicea*. Below it follows the Irano-Turanian vegetation zone on the upper slopes towards the Dead Sea, dominated by steppe grasslands with *Artemisia herba-alba* and other plants. Below this belt, the Saharo-Arabian vegetation zone with salt-tolerant Chenopodiaceae and *Tamarix* spp. grows in desert conditions. Inside this belt are azonal patches of Sudano-Deccanian vegetation, linked to freshwater springs (Zohary 1962; Davies and Fall 2001; Albert et al. 2004; Neumann et al. 2010; Langgut et al. 2015). "Palm Terrace" is such an example of azonal vegetation distribution. While situated in the Saharo-Arabian zone, it also includes wetland-adapted plants belonging to Sudano-Deccanian vegetation such as *Phoenix dactylifera*, and to Mediterranean and Irano-Turanian vegetation such as *Typha domingensis* and *Saccharum ravennae*.

## Materials and methods

### Vegetation mapping of the study site, surface pollen samples

To reconstruct the vegetation history and to investigate the long-term response of plant communities to past climatic changes and disturbances, it is crucial to understand the linkage between today's vegetation and the palynological signal that it produces. To our knowledge, no data exist about the palynological representation of oasis vegetation in the Jordan valley, although vegetation zones along an altitudinal transect could be distinguished by modern pollen precipitation (Davies and Fall 2001). In February 2016, we determined plant occurrence and abundance in 123 relevés (survey areas) of ~ 100 $m^2$ (Braun-Blanquet 1964) and collected six surface soil samples that were later analysed for pollen composition. The vegetation results were mapped using a Garmin eTrex Summit GPS receiver with an accuracy of ± 10 m and summarized on a satellite image (Google Earth 2004; Fig. 3; ESM Fig. 1). The elevation in m b.s.l. was calculated from a local coordinate system derived from total station surveying, which was carried out by a Jordanian topographical survey team, surveyor Yehya Suleiman Al-Hasanat.

### Coring and sampling

In March 2015, the 197 cm long sediment core PT1 from the centre of the "Palm Terrace" mire (31°32′14.78″N, 35°33′44.13″E) was taken with a Russian peat corer with a 5 cm diameter. To support the results from this peat core and to better understand past oasis dynamics, the 246 cm long sediment core PT2 was retrieved in February 2016 a few metres outside the active mire (31°32′16.06″N, 35°33′45.86″E) using the same coring technique. The distance between the cores is ~ 65 m. Both cores were subsampled for pollen, microscopic charcoal and macroscopic plant remains. Core PT1 provided terrestrial plant material suitable for radiocarbon dating and 34 subsamples for pollen and microscopic charcoal analyses (1 $cm^3$; at 186 and 170 cm: 2 $cm^3$) were taken between 194 and 7 cm depth with an average distance of ~ 6 cm between samples (Table 1). From core PT2, 10 subsamples (1 $cm^3$) were taken between 240 and 30 cm depth.

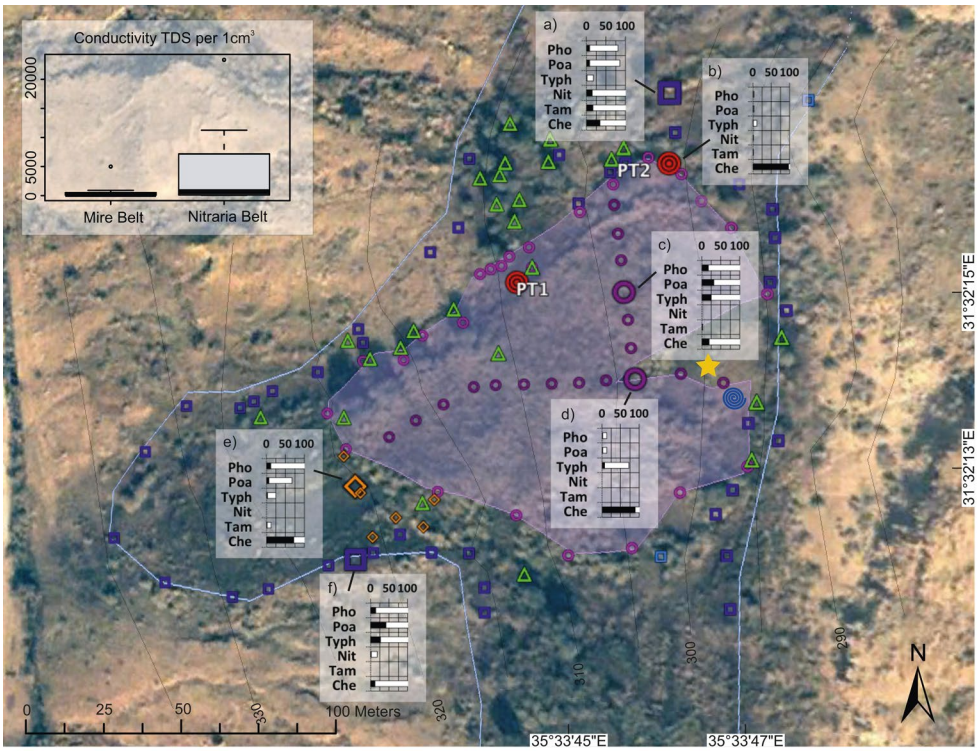


**Fig. 3** Map of "Palm Terrace" showing vegetation surveys, surface pollen samples and conductivity. Red circles indicate the coring sites PT1 and PT2. Magenta circles show vegetation plots from the outer limits of present active mire, purple circles vegetation plots on a transect through the mire. Dark blue squares show the vegetation plots from the outer limits of the *Nitraria* belt, light blue squares the additional plots in the *Nitraria* belt. Orange diamonds show vegetation plots from the outer limits of a *Phragmites* zone. Green triangles represent single palm trees (*Phoenix dactylifera*). The blue spiral shows the location of an active spring. The yellow star indicates a small zone that was heavily influenced by grazing. Large symbols indicate the position of surface pollen percentage diagrams [selected types: *Phoenix dactylifera* (Pho), Poaceae (Poa), *Typha domingensis*-type (Typh), *Nitraria retusa* (Nit), *Tamarix nilotica* (Tam), Chenopodiaceae/Amaranthaceae (Che)], the white bars show ×10 exaggerations. The conductivity diagram shows the total dissolved solids (TDS) per 1 $cm^3$ on a logarithmic scale from surface samples taken either inside the active mire or inside the *Nitraria* belt. Vertical thin lines indicate the topography (m b.s.l.)

**Table 1** Radiocarbon dates and calibrated ages from core PT1

| Lab. code | Depth (cm) | Material | $^{14}$C Age (uncal BP[a]) | Age 2σ range (cal AD) | Age in diagram (cal AD) |
|---|---|---|---|---|---|
| BE-2647.1.1 | 60–64 | Rhizome | Modern | Rejected | – |
| BE-5610.1.1 | 65.5 | Charcoal | 225 ± 50 | 1516–1955[b] | 1628 |
| BE-2648.1.1 | 93.5 | Charcoal | 695 ± 40 | 1255–1392 | 1388 |
| BE-2649.1.1 | 151–153.5 | Charcoal | 770 ± 70 | 1047–1390 | 1164 |

Calibration according to the IntCal13 Northern Hemisphere atmospheric radiocarbon calibration curve (Reimer et al. 2013)

[a]Following Stuiver and Polach (1977)

[b]Postbomb for Northern Hemisphere Region 2 (Hua et al. 2013)

## Chronology

Three samples of macroscopic charcoal (each composed of several particles > 200 µm) and a rhizome from PT1 were dated by accelerated mass spectrometry (AMS) $^{14}$C analysis in the LARA AMS laboratory of the University of Bern (Szidat et al. 2014, Table 1; Fig. 4). For calibration of the $^{14}$C dates, the IntCal13 Northern Hemisphere atmospheric radiocarbon calibration curve (Reimer et al. 2013) and the post-bomb curve for the Northern Hemisphere Region 2 (Hua et al. 2013) were used. The date of the rhizome was not used for any of the calculations of the age-depth model,

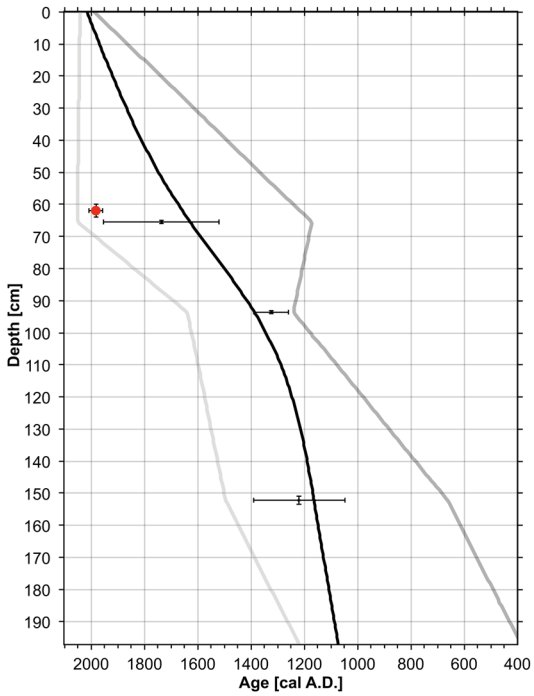


**Fig. 4** Age-depth diagram for "Palm Terrace" 1 (PT1). Black dots represent the three calibrated radiocarbon ages from macroscopic charcoal (Table 1), with error bars for vertical thickness of the samples and 2σ for estimated age (Calib 7.1, Reimer et al. 2013). The model (smooth spline 0.3, black line) was developed with the program clam 2.2 (Blaauw 2010), the outer lines show the 95% confidence envelope of the generalized mixed-effect regression (Birks and Heegaard 2003). The red dot shows the dated rhizome that was not included in the model calculations

because we assume that it had penetrated into older layers, which would explain its modern age. The smooth-spline curve of the age-depth model (Fig. 4, smooth-spline 0.3) was computed with the program clam 2.2 (Blaauw 2010); the 95% confidence envelope was calculated according to generalized mixed-effect regression (Birks and Heegaard 2003).

## Palynological analysis, presentation of results and zonation of the pollen diagram

Abundant pyrite framboids occurred in the sediments, especially in the deeper parts of the two cores, which made it very hard to extract pollen with standard laboratory methods. We therefore applied two different pollen preparation methods depending on pyrite content (Rambeau et al. 2015). Samples with low pyrite content and the surface samples were treated chemically with the standard method using HCl, KOH, HF, sieving over 0.5 mm, decanting, acetolysis and storage in glycerine (Moore et al. 1991). Samples with high pyrite content (PT1: 194, 187, 178, 171, 162, 154, 145, 138, 130, 126, 122 cm; PT2: 228, 216 cm) received a different treatment with $HNO_3$ instead of acetolysis (Rambeau et al. 2015). To calculate particle concentrations (particles $cm^{-3}$) and influx (particles $cm^{-2}$ $year^{-1}$), *Lycopodium* tablets with a known number of spores were added prior to processing (Stockmarr 1971). The pollen reference collection of the University of Bern together with pollen keys and atlases (Reille 1992, 1995, 1998; Moore et al. 1991; Beug 2004; Phillips et al. 2013) were used for identifying pollen and spores under a light microscope at 400× magnification. Because of extremely low pollen and spore abundances and the very poor preservation towards the deeper ends of the two cores, the minimum pollen sum was only 51 in PT1, while no pollen was detected in the deepest samples of core PT2. The average pollen sum in PT1 was 148. In the remaining samples of PT2, the pollen sum varied between 57 and 704, with an average of 170 pollen grains per sample. In the six surface samples, an average of 347 pollen grains was counted per sample. Since wetland plants such as *T. domingensis, Phragmites australis* and other members of the Poaceae are the dominant components of the oasis vegetation and the main contributors to the pollen signal, their pollen was included in the pollen sum, whereas algae and fungal spores were excluded. Chenopodiaceae/Amaranthaceae (Cheno/Ams) were put in the herb sum, although this taxon includes some shrubs. The pollen diagrams were drawn with Tilia 2.0.41. Local pollen assemblage zones (LPAZ) were identified by optimal sum of squares partitioning (Birks and Gordon 1985) using ZONE v.1.2 (Juggins 1991), and their statistical significance was tested with BSTICK (Bennett 1996). No statistically significant LPAZs were found in PT1 when the wetland plants were included. To find out if upland vegetation history could be subdivided into statistically significant LPAZs, we excluded the wetland plants from the pollen sum and repeated the zonation procedure. Although exclusion of wetland plants has the disadvantage of lowering the pollen sums, this procedure yielded five statistically significant LPAZs (Figs. 5, 6). In PT2 the same analysis, with wetland plants included, revealed two statistically significant LPAZs (Fig. 7). Microscopic charcoal particles (> 10 µm) were analysed in core PT1 following standard methods and presented as concentrations and influxes (Fig. 6; Tinner and Hu 2003; Finsinger and Tinner 2005). All palynological data derived from this study are presently stored in the Alpine Palynological Database (ALPADABA).

The programs CANOCO 4.5 and CanoDraw 4.14 (Lepš and Šmilauer 2003) were used for ordinations. For the vegetation survey and the surface samples, detrended correspondence analysis (DCA) was carried out with detrending by second order polynomials (Fig. 8). Since the gradient lengths of DCA axis 1 were smaller than 2.5 standard deviations in PT1 and PT2 (Legendre and Birks 2012), we decided to use the linear response model of principal component analysis (PCA) for the records (Figs. 5, 8, 9).

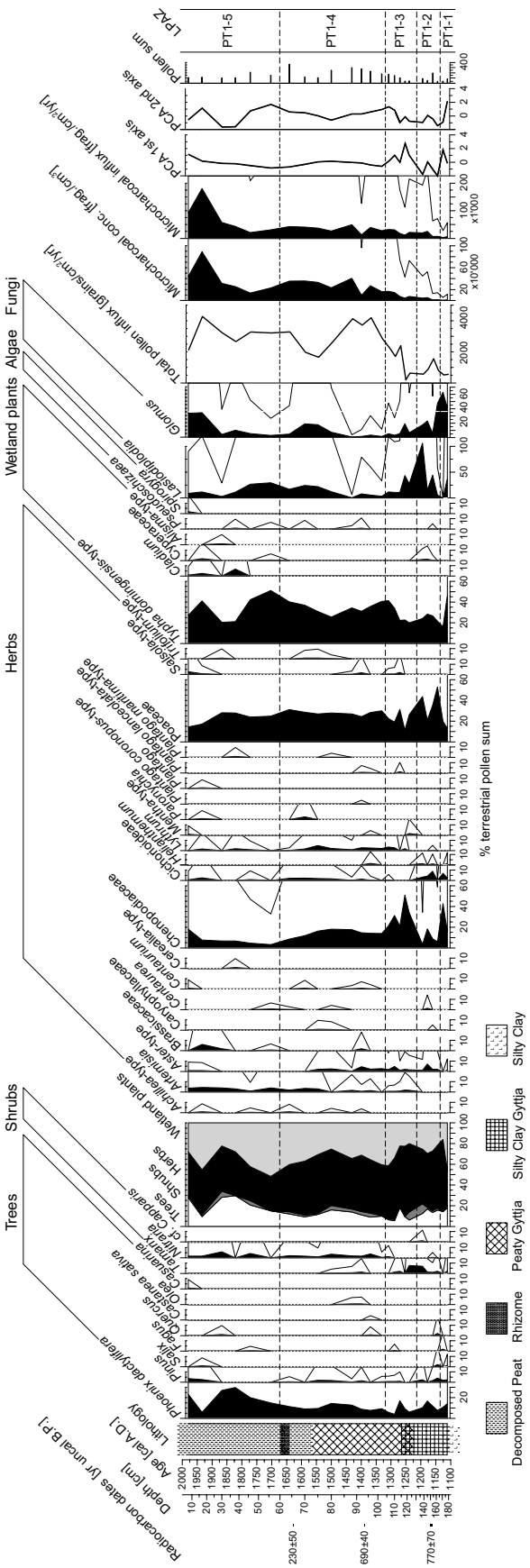


**Fig. 5** Lithology, pollen and spore percentages, microscopic charcoal concentrations (particles > 10 µm/cm$^3$) and influx (particles/cm$^2$/year) from "Palm Terrace" 1 (PT1). Sample scores of PCA axis 1 and 2 are used to summarize the vegetation dynamics. Empty curves show ×10 exaggerations. *LPAZ* Local pollen assemblage zone (statistically significant when excluding wetland plants)

### X-ray fluorescence (XRF) analysis, loss on ignition and conductivity

XRF analysis was performed on PT1 and PT2 at the Institute of Geological Sciences, University of Bern, using an Itrax core scanner (Cox Analytical System) equipped with a Mo tube (30 kV, 40 mA) at 1 cm resolution and an analysis time of 20 s per measurement. The lines were smoothed by applying a 5 point moving average, and only values with a mean squared error (MSE) lower than 3 were taken into consideration. The top 50 cm sediment of PT1 was accidentally lost before analysis, so that XRF and other data are missing for this part.

Loss on ignition (LOI) was performed on 23 samples of 1 cm$^3$ from PT1 and 8 from PT2, after drying the samples > 24 h at 105 °C, in a muffle furnace at 550 °C and then 950 °C (Heiri et al. 2001). To estimate changes in total dissolved solids, relative conductivity measurements were performed on 2 cm$^3$ sub-samples from 35 surface samples, seven samples from PT1 and eight samples from PT2. These were diluted in 20–400 ml of distilled water and the conductivity of the solution was then measured (HANNA HI 98129) and converted to total dissolved solids (TDS) in the solution, as parts per million (ppm) per 1 cm$^{-3}$ of sediment (Figs. 3, 9).

## Results and interpretation

### Vegetation survey and surface samples

The map of the oasis (Fig. 3) together with the ordination of the vegetation survey (Fig. 8a) show spatial and statistical separation into two main vegetation belts: wetland vegetation in the mire with *T. domingensis* and *P. australis*, and drought-adapted upland vegetation around the mire with *Nitraria retusa* and Chenopodiaceae. In between these two vegetation types were scattered *P. dactylifera* palms. In large oases elsewhere, *Phoenix* can form a mesophilous date palm belt between wetland and drought-adapted vegetation (Horowitz 1992). The moisture gradient at "Palm Terrace" is probably too steep and spatially too undefined to allow a distinct palm belt to grow, but the spatial distribution of the single palms between the wetland and the drought-adapted vegetation (Fig. 3, green triangles) argues for the presence of

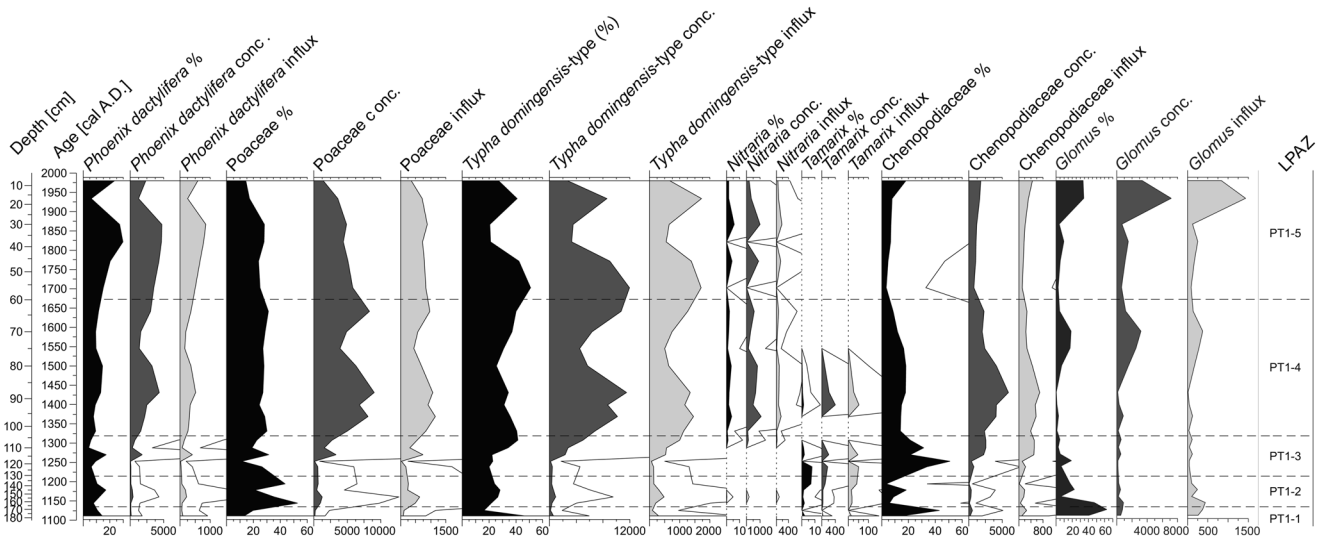


**Fig. 6** Comparison between pollen percentages (black), concentrations (pollen grains/cm$^3$, dark grey) and influx (pollen grains/cm$^2$/year, light grey) of selected pollen types from core PT1. Empty curves show ×10 exaggerations

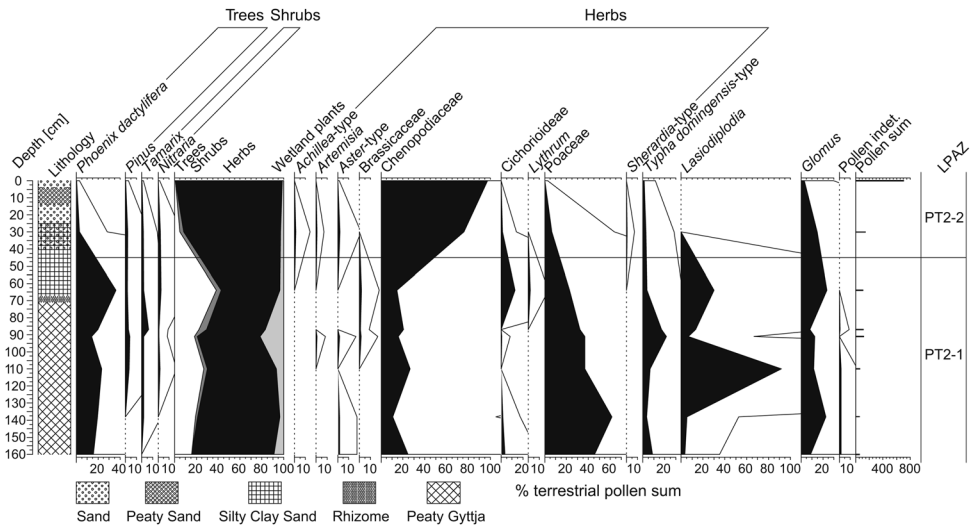


**Fig. 7** Lithology, selected pollen and spore percentage diagram from core "Palm Terrace" 2 (PT2) plotted on a depth scale. Empty curves show ×10 exaggerations. *LPAZ* local pollen assemblage zone (statistically significant including wetland plants)

a perhaps relict *P. dactylifera* ecotone zone (see vegetation history section).

The mire vegetation (Fig. 3, magenta/violet circles, ESM Fig. 1) was dominated by *Saccharum ravennae, P. australis* and in the wettest places *T. domingensis*, all of which are hydrophytes (Danin and Orshan 1999). These species are common indicators of flowing water (Danin and Orshan 1999). *S. ravennae* and *T. domingensis* are characteristic of fresh water, whereas *P. australis* also grows in slightly saline water (Danin 1983). Outside the mire under mesophilous conditions, *P. dactylifera, Tamarix nilotica, Juncus maritimus* and *Imperata cylindrica* were the most common species. *Nitraria retusa* formed an eponymous belt at the outermost limit of the oasis vegetation (Fig. 3, blue squares). It is drought-adapted and highly salt-tolerant (up to 56 dS/m, Al-Oudat and Qadir 2011), as is also the more mesophilous *T. nilotica*, which can accumulate salt in its leaves and excrete it again, which can then increase the salinity of the surface soil (Decker 1961; Mozingo 1987; Al-Oudat and Qadir 2011). Drought-adapted Chenopodiaceae are the dominant plants in the upland vegetation around the mire.

Desert springs are considered to be the natural habitat of the mesophilous date palm, *P. dactylifera* (Danin 1983). The palm is reported to need a high freshwater table (Danin and Orshan 1999), although it frequently grows on moist saline soil with a salt crust, if the roots can penetrate to less saline water beneath (Danin 1983). The distribution of the vegetation together with the topography of the oasis points

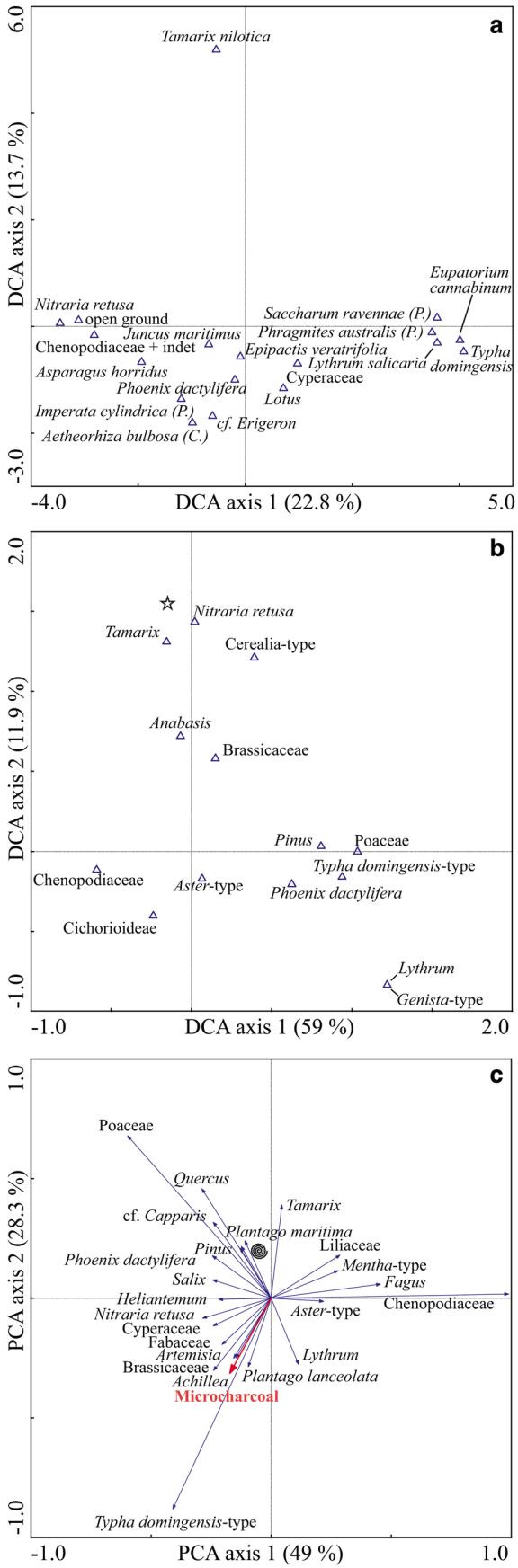


**Fig. 8** Species plots from the ordination analysis. **a** DCA of the vegetation surveys, axis 1 explains 22.8% of the variance in the data set and axis 2 explains 13.7%. "Chenopodiaceae + indet" includes Chenopodiaceae/Amaranthaceae and other plants that were unidentifiable, flowerless and often desiccated. (P.) after the name stands for the family of Poaceae, (C.) for the sub-family Cichorioideae. **b** DCA of the surface pollen samples, where axis 1 and 2 explain 59 and 11.9% of the data variance, respectively; the star represents a group of pollen types that only appear in one sample, namely *Allium, Centaurea, Centaurea scabiosa*-type, *Cucumis sativa, Daucus*, cf. *Frankenia, Plantago maritima*-type, *Polygonum alpinum*-type, *Quercus, Salix* and *Solanum nigrum*. **c** PCA of the pollen samples from PT1, 1st axis explains 49% of the variation, 2nd axis 28.3%, only the pollen types with values > 0.2 are shown, as well as the microscopic charcoal influx; the following group of pollen types are represented as a spiral: *Alisma*-type, *Astragalus, Calendula, Carlina* and Cerealia-type

to an inflow of fresh water close to the eastern border of the mire. This is confirmed by finding a spring with many young seedlings of *P. dactylifera* close to the eastern limit of the mire (Fig. 3). In general, a negative relationship between percentage seed germination and salt concentration has been observed for *P. dactylifera* (Ramoliya and Pandey 2003; Alhammadi and Kurup 2012).

Date palms are dioecious, and only a few pollen-producing male trees are needed for date production, i.e. a male–female ratio ~ 1:50 (Jain et al. 2011; Chao and Krueger 2007). Uncultivated stands are characterized by a higher proportion of males, the occurrence of trees with clustering trunks (Jain et al. 2011) and abundant *J. maritimus* var. *arabicus*, which is also very salt tolerant (> 56 dS/m, Al-Oudat and Qadir 2011), in the undergrowth (Danin 1983). The palm stands in the marginal zone of "Palm Terrace" fulfilled these criteria to a fair degree, suggesting that these dates were not cultivated for food.

DCA axis 1 of the vegetation survey shows a water availability gradient and groups the wetland plants *T. domingensis, Eupatorium cannabinum, Lythrum salicaria, S. ravennae* and *P. australis* opposite to *N. retusa*, Chenopodiaceae and "open ground", whereas mesophilous taxa such as *T. nilotica, P. dactylifera* and *J. maritimus* are located in an intermediate position (Fig. 8a). On DCA axis 2 *T. nilotica* is distant from the rest, pointing to a salinity gradient within the mesophilous vegetation. Conductivity measurements on the surface soil samples indicate an increasing salinity from the centre towards the edge of the oasis with increasing salinity down the slope and with increasing distance from the freshwater inflow at its eastern edge (Fig. 3).

Modern pollen surface samples together with present-day vegetation surveys are the key for the interpretation of past vegetation changes from pollen sequences (Baruch 1993; Davies and Fall 2001; Lopez-Merino et al. 2016). The results from six pollen surface samples are presented as pollen percentages (Fig. 3) as well as concentrations (ESM Fig. 2) and compared to the present-day vegetation using

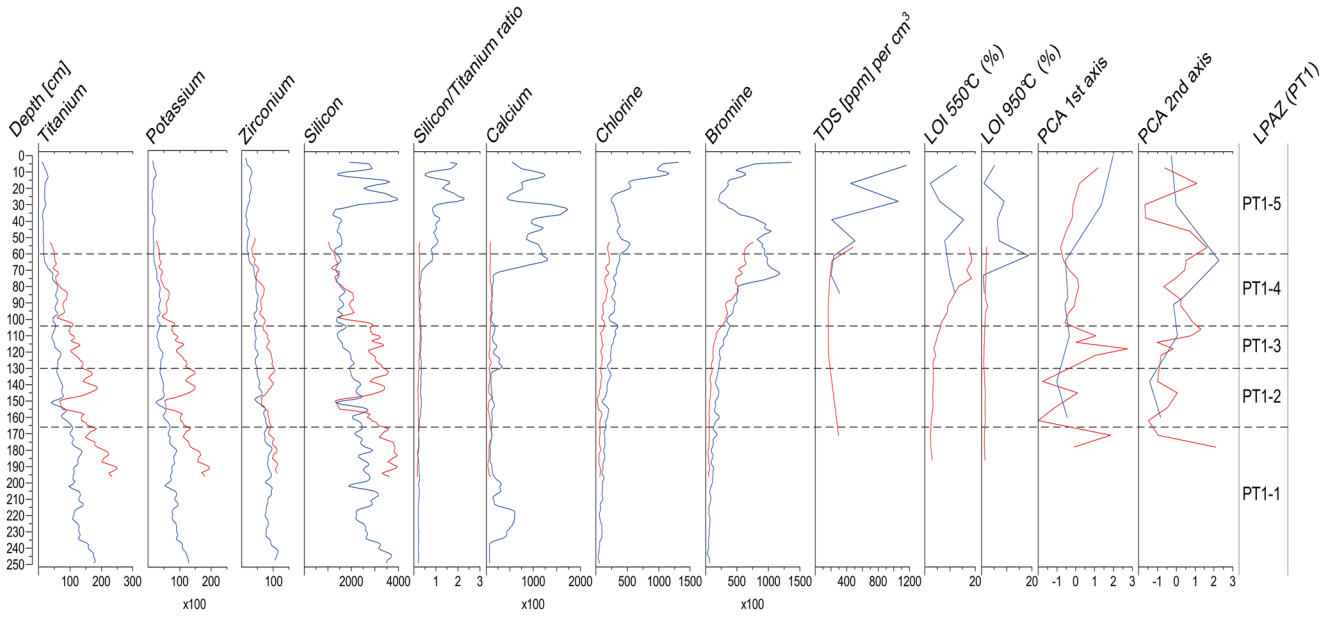


**Fig. 9** X-ray fluorescence (XRF) raw counts; titanium, potassium, zirconium, silicon, silicon/titanium ratio, calcium, chlorine and bromine, relative conductivity (TDS), loss on ignition (LOI) and Principal Component Analysis (PCA) from the pollen data of the two cores PT1 (red) and PT2 (blue) plotted against depth. Dashed lines indicate local pollen assemblage zones (LPAZ) from PT1

ordination (Fig. 8a, b). On DCA axis 1, Chenopodiaceae/Amaranthaceae (Cheno/Ams) pollen figures as the main opponent to *T. domingensis*-type and Poaceae (including *P. australis* and *S. ravennae*) pollen (Fig. 8b). In samples b, d and e, dominance of Cheno/Ams pollen (up to 98% in b, Fig. 3) may have suppressed the percentage representation of other taxa, considering that concentrations of these taxa are relatively high (ESM Fig. 2). 27.5% of all halophytic taxa in the Mediterranean basin belong to the Chenopodiaceae family (Shaer and Squires 2015). The interpretation of this family is, however, problematic due to the huge variety of different taxa which grow in the region, including annual herbs but also shrubs with distinct ecologies (Zohary and Feinbrun-Dothan 1966; Horowitz 1992). In the pollen surface samples, the highest concentration of *T. domingensis*-type pollen was found in the innermost sample of the mire (d), where neither *N. retusa* nor *T. nilotica* pollen were detected (Fig. 3). The most abundant pollen types in the outermost samples on the northern side of the oasis were Cheno/Ams, *N. retusa, T. nilotica* and *P. dactylifera* (Fig. 3a, b). These results show that pollen assemblages from oasis surface samples generally represent local vegetation accurately. If dated, sediment samples from deeper layers may thus provide useful insights into long-term vegetation dynamics. It is important, however, to keep in mind that Cheno/Ams might be somewhat overrepresented in the local pollen records due to the great abundance of the plants in the surrounding upland vegetation. Conversely, certain taxa such as *Nitraria* and *Tamarix* might be underrepresented.

## Chronology

The age-depth model for core PT1 (Fig. 4) is based on three calibrated $^{14}$C dates from charcoal samples (Table 1) and dates back to ca. AD 1100, although the 95% confidence envelope, which considers both age and depth uncertainties (Birks and Heegaard 2003), indicates that the bottom of the record might be significantly older (AD 390). Our interpretations are based on the most likely age (Fig. 4, black line), but they consider the large uncertainties that are inherent in the dating approach. During the past ~1,000 years the model suggests that there were only small changes in sedimentation rates. From bottom to top, sedimentation rates are relatively high (0.4 cm year$^{-1}$) until 140 cm depth, when they decrease to 0.1 cm year$^{-1}$ at 80 cm depth and then slightly increase again to 0.2 cm year$^{-1}$ at the top of the core. This is also reflected in pollen concentrations, with low values in the lowermost part of the record (Fig. 6). No date could be obtained from core PT2 due to the lack of suitable terrestrial macrofossils.

## "Palm Terrace" 1, vegetation and fire history according to pollen and charcoal

The pollen diagram of core PT1 shows five local pollen assemblage zones (LPAZ, Figs. 5, 6, 9; ESM Fig. 3). The pollen zones are statistically significant when pollen from wetland plants is excluded from the pollen sum. This finding suggests that only minor changes occurred in wetland

vegetation, whereas upland vegetation significantly varied over time. Poaceae are not considered as limited to wetlands because some species such as *I. cylindrica* were also common outside the mire. Nevertheless, we assume that most Poaceae pollen derives from *P. australis* and *S. ravennae*, both of which were dominant in the mire.

In LPAZ PT1-1 (AD ~ 1100 to ~ 1130), high percentages of herb pollen, mainly Cheno/Ams and Cichorioideae, point to a well-developed upland vegetation belt. *Phoenix dactylifera* pollen indicates the presence of mesophilous date palm stands. The high percentage of *T. domingensis*-type (up to 50%) suggests that it dominated the wettest part of the mire. The extremely high values of *Glomus* fungal fruiting bodies may derive from soil erosion (Anderson et al. 1984; van; Geel 1986; Kołaczek et al. 2013). Low microscopic charcoal concentrations and influx values suggest low fire activity in the region.

The continuous and increasing pollen curve of *T. nilotica* as well as the first grains of *N. retusa* suggest an expansion of salt-tolerant vegetation with shrubs in LPAZ PT1-2 (AD ~ 1130 to ~ 1220). Single finds of *Capparis* pollen indicate the presence of this typical Mediterranean shrub. Percentages of over 10% *Glomus* fruiting bodies again point to soil instability. Pollen percentages of *P. dactylifera* remain at ca. 10%, suggesting unchanged abundance of this palm in the oasis. Wetland plant sums are lowest in this zone, indicating lower water availability compared to the rest of the sequence. *Lasiodiplodia* fungal spores are abundant, pointing to infestation by this plant pathogen at or close to the site. The slight rise in microscopic charcoal suggests that fire activity marginally increased in the catchment of the oasis.

LPAZ PT1-3 (AD ~ 1220 to ~ 1320) is characterized by a strong rise in Cheno/Ams pollen percentages, peaking in this pollen zone. This suggests expansion of drought-adapted upland vegetation, mainly at the cost of wetland vegetation, which has low values, and mesophilous *T. nilotica* (Fig. 6). In agreement, pollen data suggest that the drought-adapted *N. retusa* expanded markedly, while mesophilous *P. dactylifera* contracted to minimum abundances (percentages, concentrations and influx). The rise in microscopic charcoal suggests increasing fire incidence.

In PT1-4 (AD ~ 1320 to ~ 1650) *T. domingensis*-type and Poaceae markedly increase, indicating a distinct expansion of wetland vegetation. Towards the end of this zone at around AD 1600, percentages of wetland plants rise further, reaching their highest values around AD 1700, pointing to a marked increase of moisture availability throughout this period. This interpretation is reinforced by a progressive expansion of *P. dactylifera* and a decline of Chenopodiaceae, suggesting that the moisture-requiring date palms expanded into the drought-tolerant vegetation belt of the oasis.

Pollen zone PT1-5 (AD ~ 1650 to today) is characterized by a major increase of moisture-demanding *P. dactylifera* percentages, suggesting a strong expansion of date palms in the oasis that peaked around AD 1850. This is also very well seen in both concentration and influx values, showing that this major vegetation change was real and not related to distortions from percentage calculation. The dominance of date palm vegetation, probably forming its own belt at "Palm Terrace", was preceded by the expansion of wetland vegetation around AD 1700–1750. Around AD 1750–1800, when conditions were moist, arable farming may have been practised at the oasis, as shown by single Cerealia-type and *Plantago maritima*-type finds. Towards the end of the zone, at AD 1900–1950 date palms declined, while fire activity and soil erosion markedly increased as shown by a microscopic charcoal peak and an increase in *Glomus* fungal fruiting bodies (Fig. 5).

Taken together, the pollen record of PT-1 shows an increasing expansion of moisture-requiring vegetation such as *T. domingensis*-type and *P. dactylifera* that came to an end during the twentieth century. These dynamics are summarized by the ordinations. In the taxa scores, the PCA axis 1 of PT1 (explaining 49% of the variance) spans along a gradient from drought-adapted Chenopodiaceae to moisture-requiring *P. dactylifera, T. domingensis*-type and Poaceae (probably dominated by *P. australis* and *S. ravennae*), and may thus primarily reflect a moisture gradient (Fig. 8c). Scores of PCA axis 1 through time can therefore be used as a moisture indicator curve (Fig. 5). PCA axis 2 (28%) mainly spans between Poaceae and *T. domingensis*-type, which is more difficult to explain. However, aligned along depth and thus with time (Fig. 5) the sample scores of PT1 show that PCA axis 1 is mainly related to Chenopodiaceae, while PCA axis 2 closely follows *T. domingensis*-type. The pollen records of these two plant taxa can thus be used to illustrate the primary vegetation dynamics of the oasis.

## "Palm Terrace" 2, vegetation history from pollen

Compared to PT1, PT2 is fragmentary and undated (Fig. 7). Nevertheless, it can be used to assess whether major vegetation patterns found at PT1 can also be detected at the edge of the oasis. Indeed, PT1 and PT2 share common biostratigraphic trends such as high Poaceae pollen percentages that decrease towards the top and a steady increase of *P. dactylifera* pollen from 160 to 45 cm (LPAZ PT2-1). The drastic increase of Cheno/Ams pollen (up to 98%) in the topmost 45 cm (LPAZ PT2-2) is associated with an almost complete disappearance of date-palm vegetation. Although more pronounced, this marked change may correspond to the date palm decline of the twentieth century in PT1, which was also linked to a minor subsequent increase of Cheno/Ams (Figs. 5, 6, 7).

## Lithology, XRF, conductivity and loss on ignition as environmental proxies

The lowermost part of core PT1 consisted mainly of silty clay, changing to a mixture of silty clay gyttja with increasing organic matter towards the top, where it gradually changed from peaty gyttja to decomposed peat (Fig. 5). The bottom of PT2 consisted mainly of sandy silt (246–230 cm) and silty clay (230–225 cm), which changed progressively into silty clay gyttja (190–165 cm; Fig. 7). Towards the upper part of the core, prominent changes in sedimentary composition could be observed, starting with peaty gyttja, overlain by silty clay gyttja up to a sand layer at the top that in some parts contained peaty constituents (Fig. 7). The greater number of lithological changes in PT2 suggests that the edge of the oasis may have been more sensitive to environmental fluctuations. In both cores, thick rhizomes were found; in PT1 at 60–64 cm (dated to recent times, Fig. 4; Table 1) and in PT2 at 67.5–71 cm depth.

The results of XRF measurements (Fig. 9) show that lithogenic elements such as titanium, potassium and zirconium generally decrease in values from bottom to top in both cores. This pattern is probably caused by a dilution of detrital components by increased organic matter contents, perhaps associated with the spread of palm tree vegetation. Silicon shows the same process, with one major difference at the top of PT2 where values rapidly increase from ~ 33 cm depth upwards (data for the upper 50 cm are missing for PT1). The silicon/titanium ratio (Fig. 9) shows that the diverging of the two curves in PT2 started already at ~ 70 cm, while the ratio remains stable for PT1 at least up to 50 cm depth. Diverging of silicon from other detrital elements may be explained by a second source for silicon, possibly originating in the surrounding sandstones and brought to the oasis, either by wind or by surface runoff. The sand layer in PT2 supports this hypothesis. The calcium curve of PT1 shows only minor fluctuations, although that of PT2 shows higher values at both the bottom and top. Calcium is difficult to interpret, since it can occur in many forms such as gypsum ($CaSO_4{\cdot}2H_2O$) and calcium carbonates ($CaCO_3$) (Vepraskas and Craft 2016). Calcium accumulations, however, may be linked in appropriate contexts to increased desiccation and/or lower water flow causing water supersaturation. Chlorine and bromine counts generally increase towards the top over the whole sequences of both cores. These are salinity indicators, and an increase can result from either higher salt content in the spring water, enhanced evaporation, or a combination of both (Croudace and Rothwell 2015; Beffa et al. 2016). The conductivity curves of PT1 and PT2 (Fig. 9) show the same increasing trend towards the top regarding chlorine, with higher values in PT2, in our relative measurements, up to 1,158 ppm per $cm^3$ of sediment. Compared to the conductivity of the surface samples (Fig. 3), especially those from the drought- and salinity-adapted *Nitraria* belt reaching up to 23,355 ppm per $cm^3$ of sediment, the values of the cores are still at a quite low level, and indicate increasing salt content towards both the soil surface and the edges of the oasis. Organic matter (OM) measured through loss on ignition (LOI 550 °C, Fig. 9) of PT1 increases towards the top up to 18.7%, while in PT2 it shows large oscillations. LOI at 950 °C from PT1 shows constant amounts of carbonates or potentially gypsum at low level, while in PT2 a sharp increase is shown at ~ 60 cm (there is a corresponding rise of calcium in the XRF measurements) suggesting more evaporation (Tiner 1999), followed by a decrease.

## Multi-proxy summary interpretation

Both cores PT1 and PT2 show an increase of arboreal pollen, mainly from palms in the last millennium, before a sharp reduction in the last ca. 100 years (Figs. 5, 7, 10). Conversely, detrital elements such as titanium and silicon continuously decrease in the last millennium, before silicon drastically increases in the last century (Fig. 9), suggesting

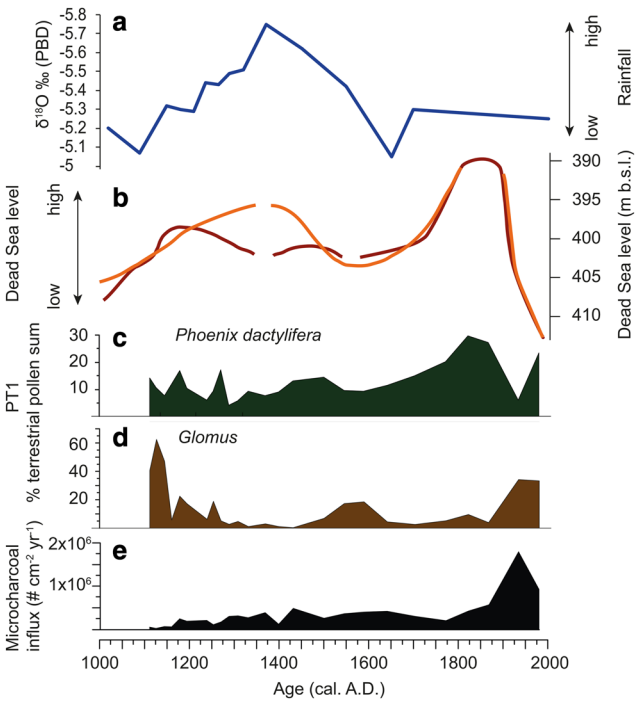


**Fig. 10** Comparison of regional palaeoclimatic indicators with vegetation, erosion and fire dynamics at "Palm Terrace". **a** $\delta^{18}O$ values from Soreq Cave speleothems as an indicator of past rainfall in the eastern Mediterranean (Bar-Matthews et al. 2003); **b** water level reconstructions of the Dead Sea from Bookman et al. (2004) (red line) and Migowski et al. (2006) (orange line); **c** pollen percentages of *Phoenix dactylifera* (date palm) as an indicator of wetland expansion; **d** percentage values of *Glomus* fungal fruit bodies as an indicator for soil erosion; **e** microscopic charcoal influx representing regional fire activity

that plant growth may have controlled the amount of mineral material brought in by erosion. Given that the presence of trees and shrubs in an oasis is primarily determined by moisture availability, these coupled bio-geosphere dynamics ultimately reflect changes in the water table. The significant change at ~ 70–60 cm depth in PT2 (ca. AD 1600–1700), at the edge of the mire, when silicon and titanium records diverge, with greater amounts of silicon, indicates an additional source of detrital input to the wetland, as well as a potential increase in evaporation suggested by higher calcium contents (PT2, Fig. 9). Chlorine counts and relative conductivity values rise drastically in the last 100 years, tracking pollen PCA axis 1 (Figs. 8c, 9), which is mainly controlled by the drought- and salinity-adapted Chenopodiaceae (Figs. 5, 6, 8, 9). At the same time, the mesophilous palm vegetation disappears, indicating a drastic change in vegetation. If we assume similar ages at similar depths in PT1 and PT2, as confirmed by the generally good litho- and chemostratigraphical (XRF) agreement between the two sequences, the wetter centre of the mire (core PT1) seems to have reacted somewhat later and less drastically, with a moderate Chenopodiaceae expansion and a less pronounced reduction of palm (Figs. 5, 6) than the drier edge in core PT2. The persistently higher abundances of the moisture-demanding halophyte *Tamarix* in core PT2 (Fig. 7) match the higher salinity reconstructions for this site at the drier edge of the oasis, as inferred from the high relative conductivity values and greater chlorine abundances (Fig. 9).

In summary, the multi-proxy evidence from PT1 and PT2 points to a drastic shrinkage of the mire and the oasis in the last ca. 100 years, probably due to less water inflow from the spring and possibly to greater evaporation shown by increased carbonate and salt contents; this is potentially linked to increased dust and/or input of eroded mineral material indicated by additional silicon-dominated detrital input, and also corroborated by the increased occurrence of *Glomus* fruiting bodies. Whereas the moisture availability was still high enough to support the mire and to some extent the palm vegetation in or close to the centre of the wetland (PT1), the mire plants and palms at the edge (PT2) were almost completely replaced by halophytes such as Chenopodiaceae, *N. retusa* and *J. maritimus*.

## Discussion

The palynological and lithological evidence suggests that the oasis vegetation was confined to a rather small area before AD ~ 1300 (Figs. 5, 6, 9, LPAZs PT1-1, PT1-2, PT1-3), to subsequently expand until ca. AD 1400–1500. Oasis vegetation temporarily contracted around AD 1500–1600, to re-expand markedly around AD 1700–1900 before the final contraction, which occurred during the past century. These oasis dynamics were most probably driven by local moisture availability.

Reconstructed water levels of the Dead Sea may be used as a proxy for regional moisture dynamics, given that these were primarily responding to changes in the balance between evaporation and precipitation (Enzel et al. 2003; Dayan and Morin 2006; Robinson et al. 2006; Bartov et al. 2007; Rambeau and Black 2011). High-resolution reconstructions by Bookman et al. (2004) and Migowski et al. (2006) (Fig. 10) suggest that Dead Sea water levels increased at AD ~ 1200, with a high level at ~ 1350, then they declined between ~ 1400 and 1600, increased again at ~ 1900 and markedly declined to 418 m b.s.l. by 2005, and then to 430 m b.s.l. in 2015 (Fig. 10; Yechieli et al. 2016). In general, these reconstructions agree well with $\delta^{18}O$ based reconstructions of rainfall from the Soreq cave speleothems, mineral deposits formed in caves (Fig. 10; Bar-Matthews et al. 2003). Considering the chronological uncertainties of our records, it is most likely that these regional moisture changes have a direct link to the environmental dynamics reconstructed at "Palm Terrace". In particular, increased regional moisture availability would explain the marked expansions of the oasis at AD ~ 1300–1500 and ~ 1700–1900 and the decreased regional moisture availability around ~ 1400–1600 would explain the contractions of the oasis wetland at ~ 1500–1700 (Figs. 5, 6, 10).

Available vegetation history reconstructions for the region (Baruch 1993; Heim et al. 1997; Neumann et al. 2007, 2009, 2010; Leroy 2010; Leroy et al. 2010; Litt et al. 2012; Langgut et al. 2014, 2015) come from the Dead Sea itself, not from local oases. The surface of the Dead Sea is, however, so large (620 $km^2$ in 2012; Ghatasheh et al. 2013) that it reflects the vegetation dynamics of a much larger regional area (Moore et al. 1991; Lang 1994), including the Mediterranean biome. Another difference is that the Dead Sea receives part of its pollen from inflowing rivers (catchment: 40,650 $km^2$, Klein and Flohn 1987), so that a regional signal with prominent *Q. calliprinos, Pistacia* and *Olea* is common (Leroy 2010; Neumann et al. 2010). The sediment record from "Palm Terrace" oasis, on the other hand, contains, with rare exceptions, only pollen of local origin, and has therefore a markedly different vegetational history, due to the absence of Mediterranean trees in the oasis. However, climatic effects on the vegetation in the Dead Sea area were reconstructed by Neumann et al. (2007) by investigating two sediment records from Ein Feshka and Ze'elim (Fig. 1). Relatively moist conditions favouring agriculture were inferred for the period ca. AD 1200–1500, followed by a short dry period after 1500, when these records end. These results also generally agree well with the phases of oasis expansion and wetland contraction at "Palm Terrace" at ~ 1300–1500 and ~ 1500–1700, respectively.

The final contraction of the oasis and the expansion of drought- and salinity-adapted vegetation (predominantly Chenopodiaceae) towards the top of our records in the centre (PT1) and particularly at the edge (PT2) of the mire might be closely connected to the drop of Dead Sea water levels which started during the twentieth century (Bookman et al. 2004; Migowski et al. 2006; Bartov et al. 2007). Lowering of Dead Sea water levels during recent decades was caused by abstraction of water from the river Jordan and from aquifer reservoirs mainly for irrigation, and from the Dead Sea itself for industrial mineral extraction (Waitzbauer 2004; Lensky et al. 2005; Abu Ghazleh et al. 2009, 2011; Chen and Weisbrod 2016; Siebert et al. 2016). The shrinkage of the Dead Sea probably causes a positive feedback of aridification, since the smaller water surface results in less evaporation from it, which reduces the air humidity in the surrounding areas and thus increasing the aridity in the region (Salameh and El-Naser 2009; Flexer and Yellin-Dror 2009; Abu Ghazleh et al. 2011). On the basis of precipitation measurements in the region from 1970 to 2002, Kafle and Bruins (2009) suggested slightly increasing trends of precipitation at the Mediterranean coast of Israel, but decreasing trends further inland. Specifically, a statistically significant decrease was observed at the meteorological station of Sedom Pans, lying next to the southern Dead Sea basin. In agreement, all Jordanian meteorological stations show decreasing precipitation trends during the last decades (Freiwan and Kadioğlu 2007). Furthermore, an abrupt and significant increase in both the mean, minimum and maximum temperatures have been observed since 1957 and 1967 (Smadi 2006), as well as a decrease in the diurnal temperature range (Freiwan and Kadioğlu 2007).

No archaeological evidence of human occupation is known that would help to assess the human legacy at the site. The map of archaeological sites around the Dead Sea provided by Beit-Arieh (1997) shows a relatively densely populated western shore, whereas on the eastern shore only a few sites at some distance north and south of the oasis are mapped. The closest archaeological finds come from Kallirrhoë, ~7 km north of "Palm Terrace" (Fig. 2), which was used as a thermal bath during Roman times, known during Byzantine times and rediscovered by Ulrich Jaspar Seetzen in AD 1807 (Seetzen 1854; Strobel 1977; Clamer and Dussart 1997; Clamer 2010). Some of the rivers described by Seetzen are, according to Kruse (in Seetzen 1854), the "Bäche Pisga" and one of them probably corresponds to the, at that time more active, "Palm Terrace" oasis. Detailed population distribution data from 1596 shows Mazra'a as the closest settlement (14 households, ~70 persons) about 20 km south of Wadi Mujib and Ras (13 households, ~65 persons) further to the east, but neither nomadic tribes nor settlements in the area of the oasis are known (Hütteroth and Abdulfattah 1977). The lack of archaeological evidence, a drastically reduced population in the area, due to the crusaders and the Black Death plague (Dols 1977; Broshi and Finkelstein 1992; Hillenbrand 2000) together with the harsh local environment let us speculate that the "Palm Terrace" area was not intensively used by humans until ~1800, when pollen of crops (Cerealia-type), ruderals (*Plantago*) and a marked increase of fire activity (charcoal) in PT1 point to human activities (Fig. 5). Of special interest is the pollen of *Casuarina*, which was found in the uppermost level; this drought-adapted tree was imported from Australia for economic purposes and is also reported in other pollen studies of the area (Horowitz 1979; Baruch 1986; Heim et al. 1997; Leroy 2010; Litt et al. 2012; Schiebel 2013).

During the past century, the human population of Jordan has increased enormously, from 225,330 inhabitants in 1922 to 7,748,000 in 2016 (Barham 1994; UN data 2016), and more water such as that of the rivers Jordan and Yarmouk was extracted, dammed or channelled; such works include the Degania dam in 1932, the King Abdullah canal in 1964 and the Unity dam in 2011 (Borchardt et al. 2016). However, we cannot assess whether the shrinkage of the "Palm Terrace" oasis was caused primarily by reduced precipitation (Kafle and Bruins 2009), or if the main driver was the Dead Sea lowering that in turn resulted in a lower ground water table in the area (Salameh and El-Naser 2000; Abu Ghazleh et al. 2011). Such a change could have caused less flow from the oasis springs (Weinberger et al. 2012; Borchardt et al. 2016) and ultimately the contraction of its vegetation. It is thus likely that land use contributed to exacerbate the effects of decreasing precipitation during the past 100 years, drastically changing the extent of the "Palm Terrace" oasis. Our results unambiguously demonstrate the high climatic sensitivity of oasis environments. Future climate in Jordan and elsewhere in the eastern Mediterranean region will probably feature a further temperature increase and a decrease in precipitation (Black et al. 2011; Christensen et al. 2013; Lelieveld et al. 2016). Together with continued water extraction, this may severely endanger oasis environments such as that of "Palm Terrace", possibly leading to their final disappearance.

## Conclusions

Surface pollen studies of oases can significantly contribute to refine vegetation history reconstructions, when linked to modern vegetation surveys. The oasis vegetation at "Palm Terrace" underwent several phases of expansion and contraction, which can be connected to previously reconstructed moisture changes in the Dead Sea area. The combination of exponentially increasing water extraction and decreased precipitation has strongly affected the environments of the oasis since the beginning of the twentieth century, leading

to a drastic contraction of the wetland. So far it is unclear whether other oases in the area suffered similar developments. Multi-proxy investigations at other oasis sites might provide further evidence of a connection between local conditions and regional trends. Our study shows that oasis studies have a high potential for clarifying vegetation dynamics at the local scale. For instance, rates of change or time lags of different taxa such as *P. dactylifera* and *T. domingensis* might be explored in detail, generating high-resolution and -precision multi-proxy series. Taxonomic improvements may help to distinguish important taxa within the Chenopodiaceae/Amaranthaceae family. Such improvements, as well as the study of other wetlands in arid contexts, may generate important knowledge to anticipate future oasis dynamics under conditions of global change.

**Acknowledgements** We gratefully thank the Jordan Royal Society for the Conservation of Nature for the permission to do fieldwork in the Mujib Biosphere Reserve. Furthermore, we are grateful to Steffen Wolters for his help with the fieldwork, Sönke Szidat for radiocarbon dating and Jean-Nicolas Haas and Walter Gams for their help with identification of the fungal spores. We would also like to thank two anonymous reviewers and the handling editor for constructive comments that greatly improved this manuscript. Funding was provided by the Swiss National Science Foundation (Grant-Nr. 136731).

## References

Abu Ghazleh S, Abed AM, Kempe S (2011) The dramatic drop of the Dead Sea: background, rates, impacts and solutions. In: Badescu V, Cathcart RB (eds) Macro-engineering seawater in unique environments. Springer, Berlin, pp 77–105

Abu Ghazleh S, Hartmann J, Jansen N, Kempe S (2009) Water input requirements of the rapidly shrinking Dead Sea. Naturwissenschaften 96:637–643. https://doi.org/10.1007/s00114-009-0514-0

Albert R, Petutschnig B, Watzka M (2004) Zur Vegetation und Flora Jordaniens. In: Enzel Y, Agnon A, Stein M (eds) New frontiers in Dead Sea paleoenvironmental research. Geological Society of America, Boulder, pp 215–229

Alhammadi MS, Kurup SS (2012) Impact of salinity stress on date palm (*Phoenix dactylifera* L.)—a review. In: Sharma P, Abrol V (eds) Crop production technologies. InTech, Winchester, pp 169–178. https://doi.org/10.5772/29527

Al-Oudat M, Qadir M (2011) The halophytic flora of Syria. International Center for Agricultural Research in Dry Areas, Aleppo

Anderson RS, Homola RL, Davis RB, Jacobson GL Jr (1984) Fossil remains of the mycorrhizal fungal *Glomus fasciculatum* complex in postglacial lake sediments from Maine. Can J Bot 62(2):325–322,328. https://doi.org/10.1139/b84-316

Barham N (1994) Entwicklung und Probleme der Landwirtschaft Jordaniens. Zeitschrift für Wirtschaftsgeographie 38:23–35

Bar-Matthews M, Ayalon A, Gilmour M, Matthews A, Hawkesworth CJ (2003) Sea-land oxygen isotopic relationships from planktonic foraminifera and speleothems in the Eastern Mediterranean region and their implication for paleorainfall during interglacial intervals. Geochim Cosmochim Acta 67:3,181–3,199. https://doi.org/10.1016/S0016-7037(02)01031-1

Bartov Y, Enzel Y, Porat N, Stein M (2007) Evolution of the Late Pleistocene Holocene Dead Sea basin from sequence stratigraphy of fan deltas and lake-level reconstruction. J Sediment Res 77:680–692. https://doi.org/10.2110/jsr.2007.070

Baruch U (1986) The Late Holocene vegetational history of Lake Kinneret (Sea of Galilee). Israel Paléorient 12:37–48. https://doi.org/10.3406/paleo.1986.4407

Baruch U (1993) The palynology of Late Quaternary sediments of the Dead Sea. The Hebrew University of Jerusalem, Hebrew (in Hebrew with English abstract)

Beffa G, Pedrotta T, Colombaroli D et al (2016) Vegetation and fire history of coastal north-eastern Sardinia (Italy) under changing Holocene climates and land use. Veget Hist Archaeobot 25:271–289. https://doi.org/10.1007/s00334-015-0548-5

Beit-Arieh I (1997) The Dead Sea region: an archaeological perspective. In: Niemi TM, Ben-Avraham Z, Gat J (eds) The Dead Sea: the lake and its settings. Oxford University Press, New York, pp 249–251

Bennett KD (1996) Determination of the number of zones in a biostratigraphical sequence. New Phytol 132:155–170. https://doi.org/10.1111/j.1469-8137.1996.tb04521.x

Beug HJ (2004) Leitfaden der Pollenbestimmung für Mitteleuropa und angrenzende Gebiete, 2nd edn. Pfeil, München

Birks HJB, Gordon A (1985) Numerical methods in Quaternary pollen analysis. Academic, London

Birks HJB, Heegaard E (2003) Developments in age-depth modelling of Holocene stratigraphical sequences. PAGES News 11:7–8

Blaauw M (2010) Methods and code for "classical" age-modelling of radiocarbon sequences. Quat Geochronol 5:512–518. https://doi.org/10.1016/j.quageo.2010.01.002

Black E, Brayshaw D, Slingo J, Hoskins B (2011) Future climate of the Middle East. In: Mithen S, Black E (eds) Water, life and civilisation: climate, environment and society in the Jordan Valley. Cambridge University Press, Cambridge, pp 51–62

Bookman R, Enzel Y, Agnon A, Stein M (2004) Late Holocene lake levels of the Dead Sea. Bull Geol Soc Am 116:555–571

Borchardt D, Bogardi JJ, Ibisch RB (eds) (2016) Integrated water resources management: concept, research and implementation. Springer, Cham

Braun-Blanquet J (1964) Pflanzensoziologie: Grundzüge der Vegetationskunde, 3rd edn. Springer, Wien

Broshi M, Finkelstein I (1992) The population of Palestine in Iron Age II. Bull Amer Schools Orient Res 287:47–60. https://doi.org/10.2307/1357138

Chao CT, Krueger RR (2007) The date palm (*Phoenix dactylifera* L.): overview of biology, uses, and cultivation. HortScience 42:1,077–1,082

Chen A, Weisbrod N (2016) Assessment of anthropogenic impact on the environmental flows of semi-arid watersheds: the case study of the lower Jordan River. In: Borchardt D, Bogardi JJ, Ibisch RB (eds) Integrated water resources management: concept, research and implementation. Springer, Cham, pp 59–83

Christensen JH, Krishna Kumar K, Aldrian E et al (2013) Climate phenomena and their relevance for future regional climate change. In: Stocker TF, Qin D, Plattner G-K et al (eds) Climate change 2013: the physical science basis. Contribution of Working Group I to the Fifth Assessment Report of the Intergovernmental Panel on Climate Change, pp 1. Cambridge University Press, Cambridge,pp 217–1,308

Clamer C (2010) Paradies am Meeresrand: Die Palastanlage von Ain ez-Zara/Kallirrhoë. In: Zangenberg J (ed) Das Tote Meer: Kultur und Geschichte am tiefsten Punkt der Erde. Zabern, Mainz, pp 113–124

Clamer C, Dussart O (1997) Fouilles archéologiques de Aïn Ez-Zâra/Callirrhoé: villégiature hérodienne. Institut français d'archéologie du Proche-Orient, Beyrouth

Croudace IW, Rothwell RG (eds) (2015) Micro-XRF studies of sediment cores. Springer, Dordrecht

Danin A (1983) Desert vegetation of Israel and Sinai. Cana Publishing House, Jerusalem
Danin A, Orshan G (eds) (1999) Vegetation of Israel, vol 1: desert and coastal vegetation. Backhuys, Leiden
Davies CP, Fall PL (2001) Modern pollen precipitation from an elevational transect in central Jordan and its relationship to vegetation. J Biogeogr 28:1,195–1,210. https://doi.org/10.1046/j.1365-2699.2001.00630.x
Dayan U, Morin E (2006) Flash flood-producing rainstorms over the Dead Sea: a review. In: Enzel Y, Agnon A, Stein M (eds) New frontiers in Dead Sea paleoenvironmental research. Geological Society of America, Boulder, pp 53–62
Decker JP (1961) Salt secretion by *Tamarix pentandra* Pall. For Sci 7:214–217
Dols MW (1977) The "black death" in the Middle East. Princeton University Press, Princeton
Enzel Y, Bookman R, Sharon D et al (2003) Late Holocene climates of the Near East deduced from Dead Sea level variations and modern regional winter rainfall. Quat Res 60:263–273. https://doi.org/10.1016/j.yqres.2003.07.011
Finsinger W, Tinner W (2005) Minimum count sums for charcoal concentration estimates in pollen slides: accuracy and potential errors. Holocene 15:293–297. https://doi.org/10.1191/0959683605hl808rr
Flexer A, Yellin-Dror A (2009) State of the art. In: Hötzl H, Möller P, Rosenthal E (eds) The water of the Jordan Valley. Springer, Berlin, pp 15–54
Freiwan M, Kadioğlu M (2007) Climate variability in Jordan. Int J Climatol 28:69–89. https://doi.org/10.1002/joc.1512
Garfunkel Z, Ben-Avraham Z (1996) The structure of the Dead Sea basin. Tectonophysics 266:155–176. https://doi.org/10.1016/S0040-1951(96)00188-6
Ghatasheh NA, Mua'ad M, Faris H (2013) Dead Sea water level and surface area monitoring using spatial data extraction from remote sensing images. Int Rev Comput Softw 8(2):892–892,897
Hect A, Gertman I (2003) Dead Sea meteorological climate. In: Nevo E, Oren A, Wasser SP (eds) Fungal life in the Dead Sea. Gantner, Haifa, pp 69–116
Heim C, Nowaczyk NR, Negendank JF et al (1997) Near East desertification: evidence from the Dead Sea. Naturwissenschaften 84:398–401
Heiri O, Lotter AF, Lemcke G (2001) Loss on ignition as a method for estimating organic and carbonate content in sediments: reproducibility and comparability of results. J Paleolimnol 25:101–110
Hillenbrand C (2000) The Crusades: Islamic perspectives. Routledge, New York
Hirschfeld Y (2006) The archaeology of the Dead Sea valley in the Late Hellenistic and Early Roman periods. In: Enzel Y, Agnon A, Stein M (eds) New frontiers in Dead Sea paleoenvironmental research. Geological Society of America, Boulder, pp 215–229
Horowitz A (1979) The quaternary of Israel. Academic, London
Horowitz A (1992) Palynology of arid lands. Elsevier, Amsterdam
Hua Q, Barbetti M, Rakowski AZ (2013) Atmospheric radiocarbon for the period 1950–2010. Radiocarbon 55:2,059–2,072
Hütteroth W-D, Abdulfattah K (1977) Historical geography of Palestine, Transjordan and Southern Syria in the late 16th century. Selbstverlag der Fränkischen Geographischen Gesellschaft in Kommission bei Palm und Enke, Erlangen
Jacobson GL, Bradshaw RHW (1981) The selection of sites for paleovegetational studies. Quat Res 16:80–96. https://doi.org/10.1016/0033-5894(81)90129-0
Jain SM, Al-Khayri JM, Johnson DV (eds) (2011) Date palm biotechnology. Springer, Dordrecht
Juggins S (1991) Zone V. 1.2. Freeware. DOS Program for the zonation (constrained clustering) of palaeoecological data. In: Steve Juggins web pages at Newcastle University. https://www.staff.ncl.ac.uk/stephen.juggins/software.htm. Accessed 5 Oct 2016
Kafle HK, Bruins HJ (2009) Climatic trends in Israel 1970–2002: warmer and increasing aridity inland. Clim Chang 96:63–77. https://doi.org/10.1007/s10584-009-9578-2
Klein C, Flohn H (1987) Contributions to the knowledge of the fluctuations of the Dead Sea level. Theor Appl Climatol 38:151–156. https://doi.org/10.1007/BF00868099
Kołaczek P, Zubek S, Błaszkowski J et al (2013) Erosion or plant succession—how to interpret the presence of arbuscular mycorrhizal fungi (Glomeromycota) spores in pollen profiles collected from mires. Rev Palaeobot Palynol 189:29–37. https://doi.org/10.1016/j.revpalbo.2012.11.006
Lang G (1994) Quartäre Vegetationsgeschichte Europas: Methoden und Ergebnisse. Spektrum Akademischer Verlag, Jena
Langgut D, Finkelstein I, Litt T et al (2015) Vegetation and climate changes during the Bronze and Iron Ages (~ 3600–600 BCE) in the southern Levant based on palynological records. Radiocarbon 57:217–235. https://doi.org/10.2458/azu_rc.57.18555
Langgut D, Neumann FH, Stein M et al (2014) Dead Sea pollen record and history of human activity in the Judean Highlands (Israel) from the Intermediate Bronze into the Iron Ages (ca 2500–500 BCE). Palynology 38:280–302. https://doi.org/10.1080/01916122.2014.906001
Legendre P, Birks HJB (2012) From classical to canonical ordination. In: Birks HJB, Lotter AF, Juggins S, Smol JP (eds) Tracking environmental change using lake sediments. Springer, Dordrecht, pp 201–248
Lelieveld J, Proestos Y, Hadjinicolaou P et al (2016) Strongly increasing heat extremes in the Middle East and North Africa (MENA) in the 21st century. Clim Chang 137:245–260. https://doi.org/10.1007/s10584-016-1665-6
Lensky NG, Dvorkin Y, Lyakhovsky V et al (2005) Water, salt, and energy balances of the Dead Sea. Water Resour Res 41:W12418. https://doi.org/10.1029/2005WR004084
Lepš J, Šmilauer P (2003) Multivariate analysis of ecological data using CANOCO. Cambridge University Press, Cambridge
Leroy SAG (2010) Pollen analysis of core DS7-1SC (Dead Sea) showing intertwined effects of climatic change and human activities in the Late Holocene. J Archaeol Sci 37:306–316. https://doi.org/10.1016/j.jas.2009.09.042
Leroy SAG, Marco S, Bookman R, Miller CS (2010) Impact of earthquakes on agriculture during the Roman-Byzantine period from pollen records of the Dead Sea laminated sediment. Quat Res 73:191–200. https://doi.org/10.1016/j.yqres.2009.10.003
Litt T, Ohlwein C, Neumann FH et al (2012) Holocene climate variability in the Levant from the Dead Sea pollen record. Quat Sci Rev 49:95–105. https://doi.org/10.1016/j.quascirev.2012.06.012
López-Merino L, Leroy SA, Eshel A, Epshtein V, Belmaker R, Bookman R (2016) Using palynology to re-assess the Dead Sea laminated sediments—indeed varves? Quat Sci Rev 140:49–66
Migowski C, Stein M, Prasad S et al (2006) Holocene climate variability and cultural evolution in the Near East from the Dead Sea sedimentary record. Quat Res 66:421–431. https://doi.org/10.1016/j.yqres.2006.06.010
Moore PD, Webb JA, Collinson ME (1991) Pollen analysis, 2nd edn. Blackwell, London
Mozingo HN (1987) Shrubs of the Great Basin: a natural history. University of Nevada Press, Reno
Neumann FH, Kagan EJ, Leroy SAG, Baruch U (2010) Vegetation history and climate fluctuations on a transect along the Dead Sea west shore and their impact on past societies over the last 3500 years. J Arid Environ 74:756–764. https://doi.org/10.1016/j.jaridenv.2009.04.015
Neumann FH, Kagan EJ, Schwab MJ, Stein M (2007) Palynology, sedimentology and palaeoecology of the late Holocene Dead

Sea. Quat Sci Rev 26:1,476–1,498. https://doi.org/10.1016/j.quascirev.2007.03.004
Neumann FH, Kagan EJ, Stein M, Agnon A (2009) Assessment of the effect of earthquake activity on regional vegetation. High-resolution pollen study of the Ein Feshka section, Holocene Dead Sea. Rev Palaeobot Palynol 155:42–51. https://doi.org/10.1016/j.revpalbo.2008.12.016
Odhiambo GO (2017) Water scarcity in the Arabian Peninsula and socio-economic implications. Appl Water Sci 7:2,479–472,492. https://doi.org/10.1007/s13201-016-0440-1
Phillips AJL, Alves A, Abdollahzadeh J et al (2013) The Botryosphaeriaceae: genera and species known from culture. Stud Mycol 76:51–167. https://doi.org/10.3114/sim0021
Rambeau CMC (2010) Palaeoenvironmental reconstruction in the Southern Levant: synthesis, challenges, recent developments and perspectives. Philos Trans R Soc A Math Phys Eng Sci 368(5):225–225,248. https://doi.org/10.1098/rsta.2010.0190
Rambeau CMC, Black S (2011) Palaeoenvironments of the southern Levant 5,000 BP to present: linking the geological and archaeological records. In: Mithen S, Black E (eds) Water, life and civilisation: climate, environment and society in the Jordan valley. Cambridge University Press, Cambridge, pp 94–104
Rambeau CMC, Gobet E, Grand-Clément E et al. (2015) New methods for the palaeoenvironmental investigation of arid wetlands, Dead Sea edge, Jordan. In: Lucke B, Bäumler R, Schmidt M (eds) Soils and sediments as archives of landscape change. (Erlanger Geographische Arbeiten 42). Fränkische geographische Gesellschaft, Erlangen, pp 147–162
Ramoliya PJ, Pandey AN (2003) Soil salinity and water status affect growth of *Phoenix dactylifera* seedlings. N Z J Crop Hortic Sci 31:345–353. https://doi.org/10.1080/01140671.2003.9514270
Reille M (1992) Pollen et spores d'Europe et d'Afrique du Nord. Laboratoire de Botanique Historique et Palynologie, Marseille
Reille M (1995) Pollen et spores d'Europe et d'Afrique du Nord. Suppl 1. Laboratoire de Botanique Historique et Palynologie, Marseille
Reille M (1998) Pollen et spores d'Europe et d'Afrique du Nord. Suppl 2. Laboratoire de Botanique Historique et Palynologie, Marseille
Reimer P et al (2013) IntCal13 and Marine13 Radiocarbon age calibration curves 0–50,000 years cal BP. Radiocarbon 55:1,869–1,887. https://doi.org/10.2458/azu_js_rc.55.16947
Rimawi O, Salameh E (1988) Hydrochemistry and groundwater system of the Zerka Ma'in-Zara thermal field, Jordan. J Hydrol 98:147–163
Robinson SA, Black S, Sellwood BW, Valdes PJ (2006) A review of palaeoclimates and palaeoenvironments in the Levant and Eastern Mediterranean from 25,000 to 5000 years BP: setting the environmental background for the evolution of human civilisation. Quat Sci Rev 25:1,517–1,541. https://doi.org/10.1016/j.quascirev.2006.02.006
Salameh E, El-Naser H (2000) Changes in the Dead Sea level and their impacts on the surrounding groundwater. Acta Hydrochim Hydrobiol 28:24–33. https://doi.org/10.1002/(SICI)1521-401X(200001)28:1<24::AID-AHEH24>3.0.CO;2-6
Salameh E, El-Naser H (2009) Retreat of the Dead Sea and its effect on the surrounding groundwater resources and the stability of its coastal deposits. In: Hötzl H, Möller P, Rosenthal E (eds) The water of the Jordan valley: scarcity and deterioration of groundwater and its impact on the regional development. Springer, Berlin, pp 247–264
Salameh E, Udluft P (1985) The hydrodynamic pattern of the central part of Jordan. Geol Jahrb 38:39–53
Sawarieh A, Hötzl H, Salameh E (2004) Hydrogeology of thermal waters from Zara-Zarqa Ma'in and Jiza areas, Jordan. In: Chatzipetros AA, Pavlides SB (eds) Proceedings of the 5th International Symposium on Eastern Mediterranean Geology, Thessaloniki, Greece, 14–20 April 2004, pp 1,564–1,567
Sawarieh A, Hötzl H, Salameh E (2009) Hydrogeology and hydrochemistry of Wadi Waleh and Wadi Zarqa Ma'in catchment, central Jordan. In: Hötzl H, Möller P, Rosenthal E (eds) The water of the Jordan valley: scarcity and deterioration of groundwater and its impact on the regional development. Springer, Berlin, pp 361–370
Schiebel V (2013) Vegetation and climate history of the southern Levant during the last 30,000 years based on palynological investigation. Universitäts- und Landesbibliothek, Bonn
Seetzen UJ (1854) Reisen durch Syrien, Palästina, Phönicien, die Transjordan-Länder, Arabia Petraca und Unter-Aegypten. Reimer, Berlin
Shaer H, Squires V (2015) Halophytic and salt-tolerant feedstuffs: impacts on nutrition, physiology and reproduction of livestock. CRC, Boca Raton
Siebert C, Rödiger T, Geyer S et al (2016) Multidisciplinary investigations of the transboundary Dead Sea basin and its water resources. In: Borchardt D, Bogardi JJ, Ibisch RB (eds) Integrated water resources management: concept, research and implementation. Springer, Cham, pp 107–127
Smadi MM (2006) Observed abrupt changes in minimum and maximum temperatures in Jordan in the 20th century. Am J Environ Sci 2:114–120
Stockmarr JE (1971) Tablets with spores used in absolute pollen analysis. Pollen Spores 13:615–621
Strobel A (1977) Auf der Suche nach Machärus und Kallirrhoe: Selbstzeugnisse und Dokumente zu einem geographischen Problem des 19. Jahrhunderts. Zeitschrift des Deutschen Palästina-Vereins 93:247–267
Stuiver M, Polach HA (1977) Discussion; reporting of C-14 data. Radiocarbon 19:355–363
Szidat S, Salazar GA, Vogel E et al (2014) 14C Analysis and sample preparation at the new Bern laboratory for the analysis of radiocarbon with AMS (LARA). Radiocarbon 56:561–566. https://doi.org/10.2458/56.17457
Tiner RW (1999) Wetland indicators: a guide to wetland identification, delineation, classification, and mapping. CRC, Boca Raton
Tinner W, Hu FS (2003) Size parameters, size-class distribution and area-number relationship of microscopic charcoal: relevance for fire reconstruction. Holocene 13:499–505. https://doi.org/10.1191/0959683603hl615rp
UN data (2016) World statistics pocketbook: Jordan. United Nations statistics division. http://data.un.org/CountryProfile.aspx?crName=JORDAN. Accessed at 30 Mar 2017
Van Geel B (1986) Application of fungal and algal remains and other microfossils in palynological analyses. In: Berglund BE (ed) Handbook of Holocene palaeoecoloy and palaeohydrology. Wiley, Chichester, pp 497–505
Vepraskas MJ, Craft CB (2016) Wetland soils: genesis, hydrology, landscapes, and classification, 2nd edn. CRC, Boca Raton
Waitzbauer W (2004) Reise durch die Natur Jordaniens. Biologiezentrum, Oberösterreichische Landesmuseen, Linz
Weinberger G, Livshitz Y, Givati A et al (2012) The natural water resources between the Mediterranean Sea and the Jordan River. Hydrological Service of Israel, Jerusalem
Yechieli Y, Abelson M, Baer G (2016) Sinkhole formation and subsidence along the Dead Sea coast, Israel. Hydrogeol J 24:601–612. https://doi.org/10.1007/s10040-015-1338-y
Zohary M (1962) Plant life of Palestine: Israel and Jordan. Ronald, New York
Zohary M, Feinbrun-Dothan N (1966) Flora Palaestina. Israel Academy of Sciences and Humanities, Jerusalem